VIC-Glacier (VIC-GL)

Description of VIC Model Changes and Upgrades

VIC Generation 2 Deployment Report

Volume 1

Markus Schnorbus

Pacific Climate Impacts Consortium

University of Victoria

Victoria, BC

February 1, 2018

Citation

Schnorbus, M.A., 2018: *VIC Glacier (VIC-GL) - Description of VIC model changes and upgrades*, VIC Generation 2 Deployment Report, Volume 1, Pacific Climate Impacts Consortium, University of Victoria, Victoria, BC, 40 pp.

About PCIC

The Pacific Climate Impacts Consortium is a regional climate service centre at the University of Victoria that provides practical information on the physical impacts of climate variability and change in the Pacific and Yukon Region of Canada. PCIC operates in collaboration with climate researchers and regional stakeholders on projects driven by user needs. For more information see http://pacificclimate.org.

Disclaimer

Acknowledgements

I gratefully acknowledge the financial support of BC Hydro. I am particularly grateful for the support and guidance from Faron Anslow (PCIC), and programming support from James Stone (UVic Coop program) and Shaham Sharifian (UVic Coop program).

Contents

List of Figures

List of Tables

1 Introduction

1.1 Background

The variable infiltration capacity (or VIC) model is a spatially distributed process-based macroscale hydrology model that solves the full 1-dimensional (i.e. vertical) water and energy balance in each computational grid element. Although physical principles and laws for the general basis of the VIC model, several processes, such as runoff and baseflow, are empirical.

The basic features of the VIC model are as follows (adapted from http://vic.readthedocs.org/en/vic.4.2.c/Overview/ModelOverview/):

1. Land surface is modelled as a grid of large, flat, uniform tiles where sub-grid variability (e.g. elevation ad land cover) is handled via statistical distributions
2. Inputs are time series (daily or sub-daily) meteorological drivers
3. Land-atmosphere fluxes and water and energy balances at the land surface are simulated at a daily or sub-daily timestep
4. Water can only enter a grid cell via the atmosphere and non-channel flow between grid cells is ignored. In other words, portions of surface or sub-surface runoff that reach the local channel network are assumed to be much greater than any portions which cross into neighbouring cells. Once water reaches the channel network it stays in the channel network.

This last feature has several consequences: grid cells are simulated independently of each other, the routing of streamflow is performed separately from the land surface simulation, using a separate model, and VIC is unable to explicitly model large (e.g. multi-grid) hydrologic features such a slakes, reservoirs, regional groundwater or large glaciers and ice fields. Further details are available at the VIC model website (http://vic.readthedocs.org/en/vic.4.2.c/).

The intended modelling domain of the Hydrologic Impacts theme at Pacific Climate Impacts Consortium covers a large area in northwestern North America (Figure 1). Of particular relevance is the fact that a substantial portion of this region contains glaciated terrain. Glaciers are sensitive indicators of climate change, and glaciers throughout western North America have generally been retreating since the end of the Little Ice Age, however, the rate of recession has accelerated over recent decades, and there is concern that rates of retreat may continue to increase with future climate change. Glaciers are important natural resources that can have a substantial influence on streamflow and water quality, both locally and downstream (Moore et al. 2009). Therefore, in an effort to simulate more skilfully the cryospheric components of the hydrologic cycle in the mountainous terrain of western Canada, PCIC has updated the Variable Infiltration Capacity (VIC) hydrologic model (Liang et al. 1994, 1996; Cherkauer and Lettenmaier 1999; Cherkauer et al. 2003; Andreadis et al. 2009) to include the capability to simulate glacier mass balance and glacier dynamics. This upgraded version of the VIC model is referred to as VIC-GL. Glacier mass balance is the vertically integrated changes in rates of accumulation and ablation and glacier dynamics is the movement, or flow, of ice under its own weight, resulting in changes in glacier shape and area. The correct simulation of both mass balance and dynamics is crucial for accurately estimating changes in glacier volume and runoff over long integration periods.

The purpose of this document is to describe and illustrate the major changes made by PCIC to the VIC model to accommodate new glacier features. This document is not a user manual. The code for the VIC GL model is located on GitHub (https://github.com/pacificclimate/VIC), which is a development fork from UW GitHub repository (https://github.com/UW-Hydro/VIC).

1.2 General Approach

In summary, the engineering and feature upgrades to the VIC model had to address the following major limitations:

1. No explicit treatment of land ice, including mass and energy balance
2. Naïve representation of sub-grid land cover and topographic variability
3. No lateral flux transfer (e.g. glacier ice) between VIC grid cells

Hence, the following major design decisions guided the general approach to upgrading the VIC model:

1. Calculate glacier mass and energy balance within the VIC model, where the purpose of the mass balance model is to calculate ice melt contributions to runoff and streamflow. The mass balance model also acts as the forcing to glacier dynamics modelling. The mass balance model requires explicit simulation of:
    a. The presence/absence of glaciers
    b. Mass and energy balance model for glacier ice
    c. Water storage and runoff from the glaciers
2. As dynamics modelling requires lateral communication between neighbouring cells, glacier dynamics must be modelled externally to VIC. Therefore, VIC is to be fully coupled to an existing glacier dynamics model, with the following constraints:
    a. Glacier dynamics runs at much lower temporal resolution (monthly or annually)
    b. Conservation of water and energy between models

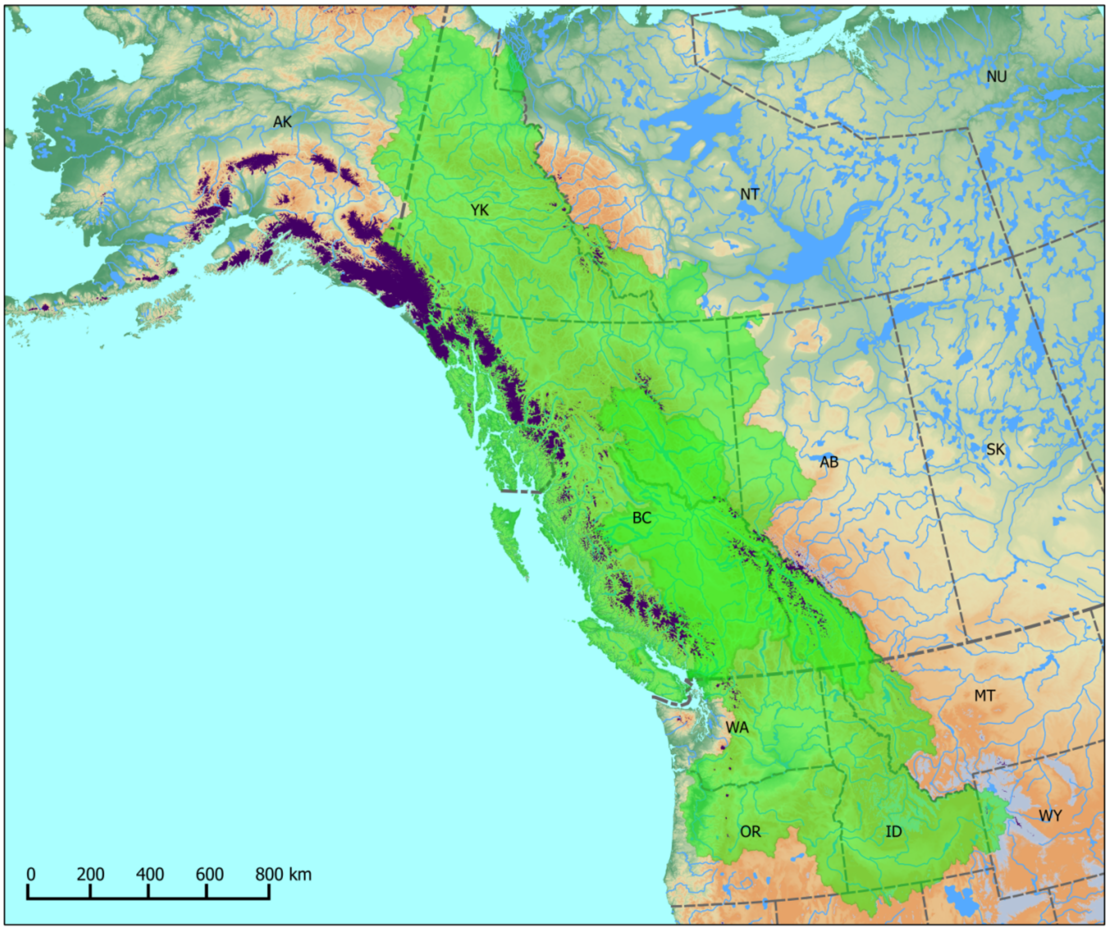

Figure 1. PCIC Hydrologic Impacts study domain (green), including glacier extent (purple), in western North America.

2 Structural Changes – Re-engineering and Factorization

VIC is a deterministic spatially distributed hydrology model, wherein the solution of the water and energy balances occurs on a computational mesh composed of rectangular grid cells. One of the major assumptions influencing the design of the original model was that energy and water fluxes do not move across cell boundaries (or more specifically, the lateral transfer of water and energy across cell boundaries is negligible and can be ignored). Hence, the original version of VIC (4.1.2) is an embarrassingly parallel model that runs in cell-major mode. Specifically, each VIC cell is run independently over the given simulation period, with separate input and output files for each grid cell. Figure 2 diagrams the main program flow for the VIC 4.1.2 model.

2.1 Minor Changes

2.1.1 Refactoring

Prior to the introduction of any major structural changes, some initial code refactoring was undertaken to remove variable aliasing and shadowing, rename variables in a consistent fashion, improve thread safety, and remove sentinel values. Lastly, the code base was converted to C++, a more modern code that allows for some design solutions, which are simpler and more elegant than the existing C-based solutions. Stone (2013) provides more details.

2.1.2 Soil Parameter File

An additional development has been to move several parameters from various places within the code base into the soil parameter file. There are two reasons for this decision: 1) to make certain parameters more accessible for model calibration and 2) to allow for a more spatially explicit description of certain hydro-climatic processes. The parameters involved are summarized in Table 1.

Table 1. Parameters moved to the soil file

Parameter	Description	Previous Location
α_o	New snow albedo	user_def.h
λ_a	Accumulation period snow albedo	user_def.h
p_a	Snow albedo accumulation exponent	user_def.h
λ_m	Melt period snow albedo	user_def.h
p_m	Snow albedo melt exponent	user_def.h
T_{TH1}	Temperature threshold parameter 1	global file
T_{TH2}	Temperature threshold parameter 2	global file
P_{adjr}	Precipitation scaling factor for rainfall	global file
P_{adjs}	Precipitation scaling factor for snowfall	global file
T_{lapse}	Temperature lapse rate (monthly values)	hardcoded
P_{grad}	Precipitation gradient	snowband file

The albedo parameters that have been moved to the soil file are only applicable for the US Army Corps of Engineers (USACE 1956) snow albedo decay algorithm (SNOW_ALBEDO = USACE in the global file). If the user selects the algorithm of Sun et al. (1999) (SNOW_ALBEDO = SUN1999 in the global file) then these values are ignored and VIC uses hard-coded parameters.

Temperature threshold parameters apply to both available algorithms (set using the TEMP_TH_TYPE in the global file). If VIC_412 is selected (original VIC algorithm; Andreadis et al. 2009) then the parameters T_{TH1} and T_{TH2} are the minimum rain temperature (air temperature below which all precipitation is rain) and maximum snow temperature (temperature above which all precipitation is snow), respectively. If the KIENZLE algorithm is chosen (Kienzle 2008, see §2.6.2), then the parameters T_{TH1} and T_{TH2} are the threshold temperature and temperature range, respectively.

The precipitation adjustment parameters P_{adj} was introduced by Schnorbus et al. (2010) as an additional calibration parameter in order to compensate for precipitation bias inherent in interpolation-based forcing data in mountainous topography. Originally added as a global parameter in the global file, it has now been moved to the soil file. A further refinement for VIC-GL is the use of separate precipitation adjustments factors for rainfall and snowfall. This is intended to capture the differences in precipitation bias between solid and liquid precipitation (i.e. due to differences in gauge undercatch), as well as differences between winter (mainly frontal) and summer (mainly convective) precipitation processes.

The temperature lapse T_{lapse} rate, which was originally hard-coded value of 6.5 °C/km, has also been added to the soil file to better reflect spatial variability from available high-resolution climatological data (i.e., PRISM).

The precipitation gradient, P_{grad}, parameter replaces the use of precipitation factors in the snowband file. P_{grad} is used to determine the climatological ratio (or precipitation factor) of precipitation in band *b* to mean grid cell precipitation as

$$\frac{P_b}{\bar{P}} = 1.0 + P_{grad}(z_b - \bar{z}) = P_{factor}(z_b) \quad (1)$$

where z_b is the elevation of band *b*, $\bar{z}$ is the mean grid cell elevation and P_{grad} is estimated from climatological data as $a/\bar{P}$, where *a* is the slope of the linear regression of precipitation on elevation

$$P = P_0 + a \cdot z. \quad (2)$$

Note that use of equation (2), which implies that precipitation increases linearly and monotonically with increasing elevation, is an over-simplification of the temporal and spatial complexities of orographic precipitation (Barry 1992; Roe 2004) that we adopt merely for computational convenience.

2.2 Code Vectorization

Sub-grid variability in the original version of VIC uses the intersection of independently specified elevations bands and land cover classes to create a two-dimensional array of tiles. These tiles then become the major computational element of the VIC model and program flow is composed of nested vegetation and elevation loops. However, this simple approach is naïve as it results in an unrealistic distribution of vegetation types with elevation (e.g., Figure 3a). In the complex mountainous topography that characterizes British Columbia, land cover and elevation tend to be dependent. In other words, certain land cover types (such as bare rock and glaciers) tend to be at high elevation, whereas forests tend to cover lower elevations (Figure 4). To model sub-grid variability more realistically, the new version of VIC collapses the two-dimensional tile array into a one-dimensional vector for describing sub-grid variability, where each element of the vector is a Hydrologic Response Unit (HRU). Unlike the original tile approach, HRUs are defined by land cover and elevation, which results in a more realistic description of sub-grid variability (Figure 3b). In an additional departure from the original tile-based approach, to allow for dynamic nature of glacier HRUs (which shrink, grow, disappear ,or appear; see Section **Error! Reference source not found.**) the size and presence of HRUs is not assumed to be fixed in time. As per the original version of VIC, the geographic locations or spatial configuration of land cover types within an elevation band is not explicit and all patches of the same cover type within an elevation band are lumped into a single HRU.

The historic use of VIC 4.1.2 typically used a maximum of five elevation bands (with approximately 500-m band relief). In VIC-GL, a much higher vertical resolution will be required to model accurately the variation of glacier mass balance with elevation (which is required for forcing a glacier dynamics model, see Section **Error! Reference source not found.**). Hence, Figure 4 also shows the difference in going from a naïve 500-m description to an explicit 100-m description of sub-grid variability. Note that the choice of elevation bands is not a structural change to the model, but a user prescription.

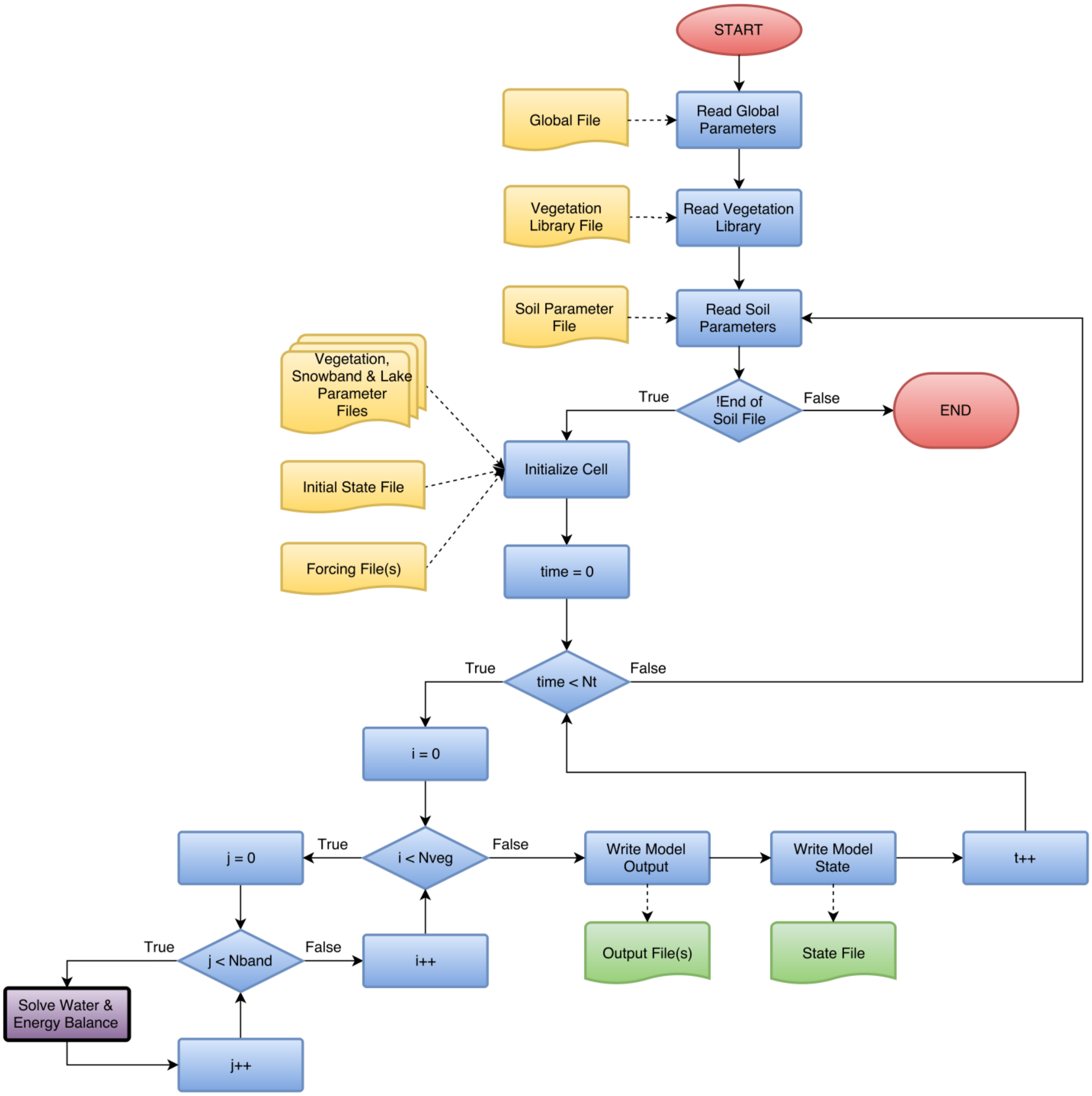

Figure 2. Main program flow for VIC 4.1.2.

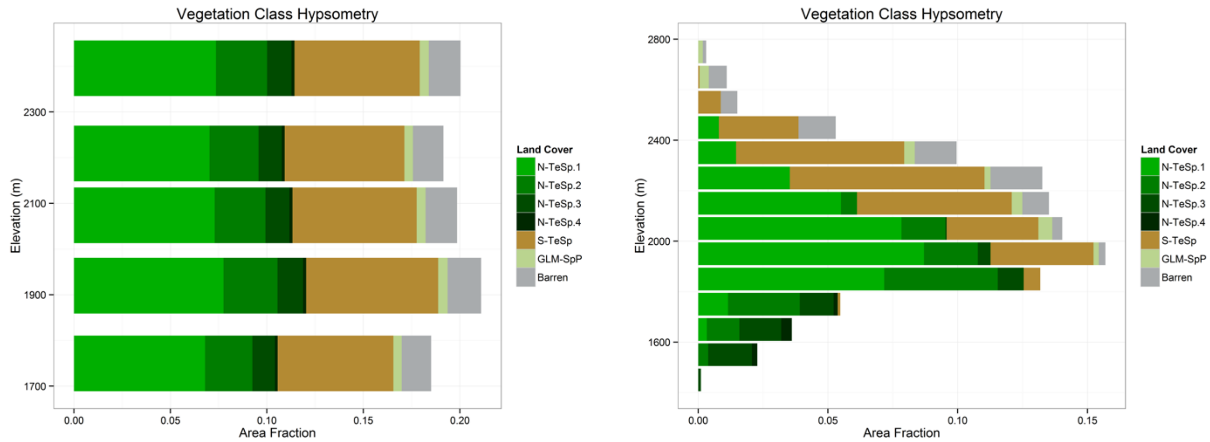

Figure 3. Graphical description of a single VIC cell using both the old and new techniques for describing sub-grid variability. Panel a) shows the original matrix-based formulation, which typically uses a maximum of five elevation bands, and panel b) shows the re-engineered vector-based approach using hydrologic response units and a much finer vertical resolution.

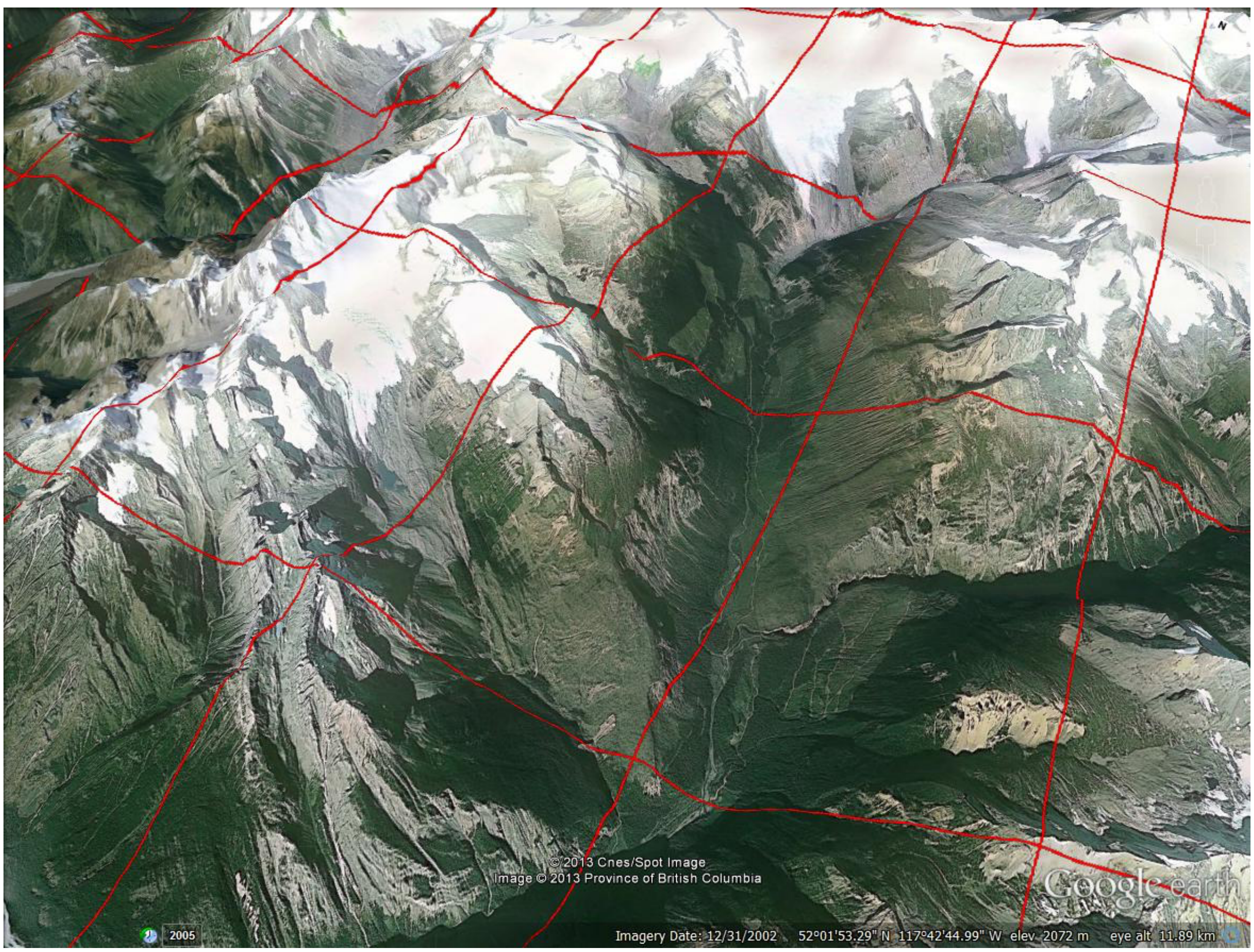

Figure 4. Example of 1/16-degree VIC computational grid draped over complex mountainous topography in British Columbia.

2.3 Updated Program Flow

2.3.1 Glacier Branch

From the perspective of computing the mass and energy balance, the model treats glaciers as static and permanent feature of the landscape. The presence or absence of glaciers on the landscape uses a specific glacier landcover type, with an explicit entry in the vegetation library file. Note that glacier area changes are dealt with in the glacier dynamics component of the model (see §**Error! Reference source not found.**). Hence, the spatial and vertical distribution of glaciers is described using the HRU structure, where all glacier-covered area within a given elevation band is treated as a single glacier HRU.

The specifics of modelling the mass and energy of glaciated terrain, which differs from the treatment of vegetated terrain, uses a separate code branch designed specifically for glacier HRUs (Figure 7). The actual mass and energy balance algorithm is described in §3.1.

2.3.2 Change to Time Major

VIC must periodically capture a 2D 'image' of model state in order to pass a mass balance forcing field to dynamics model for the entire study domain. This requirement is encumbered by VIC's original cell-major program flow (all time steps for given cell, i.e. Figure 2) and the code was restructured to loop in time major (all cells for given time step; Figure 7). Time major program flow is also more compatible (and memory efficient) with respect to writing program output to a single netCDF file (see §2.5)

2.3.3 Code Parallelization

The increase in both model complexity (particular the inclusion of glacier dynamics) and sub-grid resolution will adversely affect model run time. A vertical resolution of 200-m or less is recommended for accurate glacier mass balance modelling (a five-fold increase in the typical 500-m resolution used in past studies) which, when used in conjunction with 22 vegetation classes, results in large HRU vectors per VIC grid cell. The need to switch from daily to a sub-daily (hourly or three-hourly) time step for model integration further compounds the high computational demand. We address the increased computational demand via code parallelization by using multi-threading for the cell loop (Figure 7). Nevertheless, we anticipate that for short simulation runs, the use of multiple processors in a shared computing environment may be counterproductive. I.e., the need for multiple cores may adversely affect queuing time, which would be particularly troublesome during model calibration, which relies on order of 10^2 to 10^3 short model runs. Thus, code parallelization is optional in VIC and chosen using the settings given in Table 2.

Table 2. Parameter settings for parallel operation.

Location	Parameter	Value
user_def.h	PARALLEL_AVAILABLE	TRUE
Global file	PARALLEL_THREADS	1 = sequential (default); 2 (or more) = number of processors for multi-threading

2.4 Order of Operations

The changes in program structure and program flow are exemplified by changes in the order-of-operations by which hydrologic fluxes and states are calculated for each grid cell.

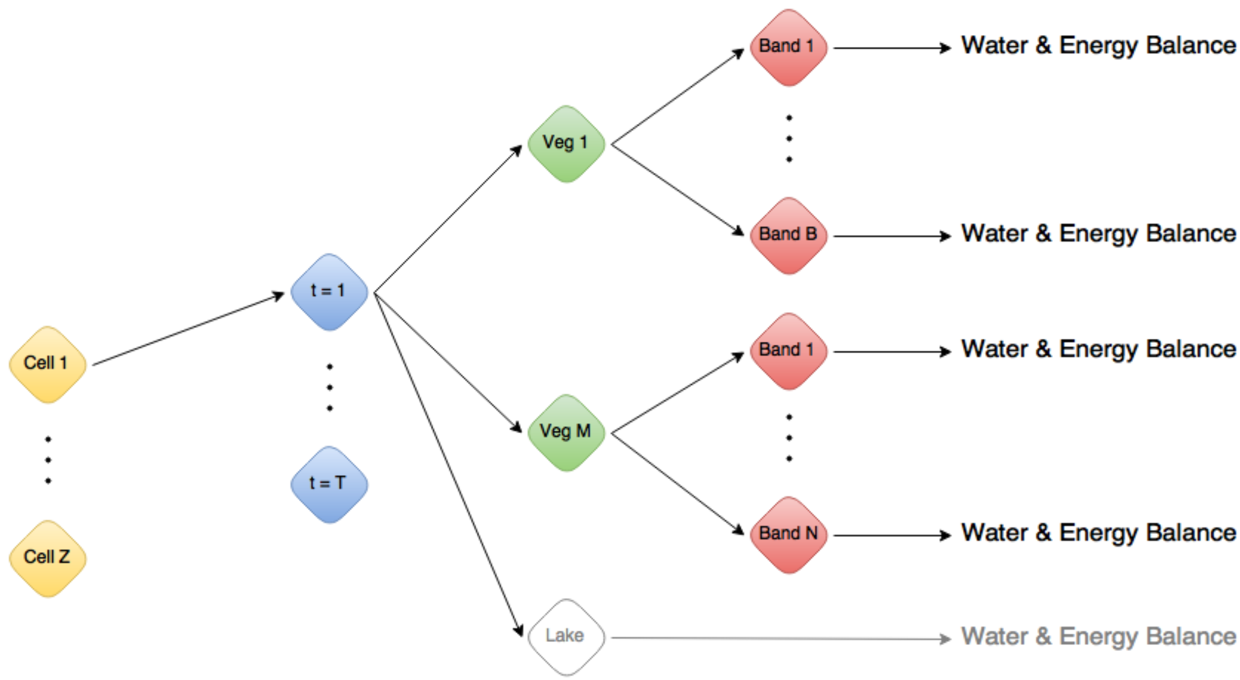

Figure 5. Order of operations for original version of VIC.

In the original version of the VIC model hydrologic fluxes and stores from individual vegetation-elevation tiles are averaged (weighted by area fraction; Figure 5) to provide a grid-cell output as

$$R[t]_{cell} = \sum_{i=1}^{M}\left[A_i \sum_{j=1}^{N}\left(A_j \cdot R[t]_{i,j}\right)\right] \tag{3}$$

where R is any given water or energy flux (or store), A_i is the area of a vegetation class i, A_j is the area of elevation band j (as grid cell fractions), t is the timestep, and M and N are the number of vegetation classes and elevation bands, respectively, in a given cell.

In the new version of VIC, sub-grid variability has been vectorized using HRUs (Figure 6) and grid-cell average hydrologic fluxes and states are now calculated as the area-weighted HRU average

$$R[t]_{cell} = \sum_{h=1}^{M}\left(A[t]_h \cdot R[t]_h\right) \tag{4}$$

where A_h is now the HRU area (as a grid cell fraction) and M is the number of HRUs per grid cell.

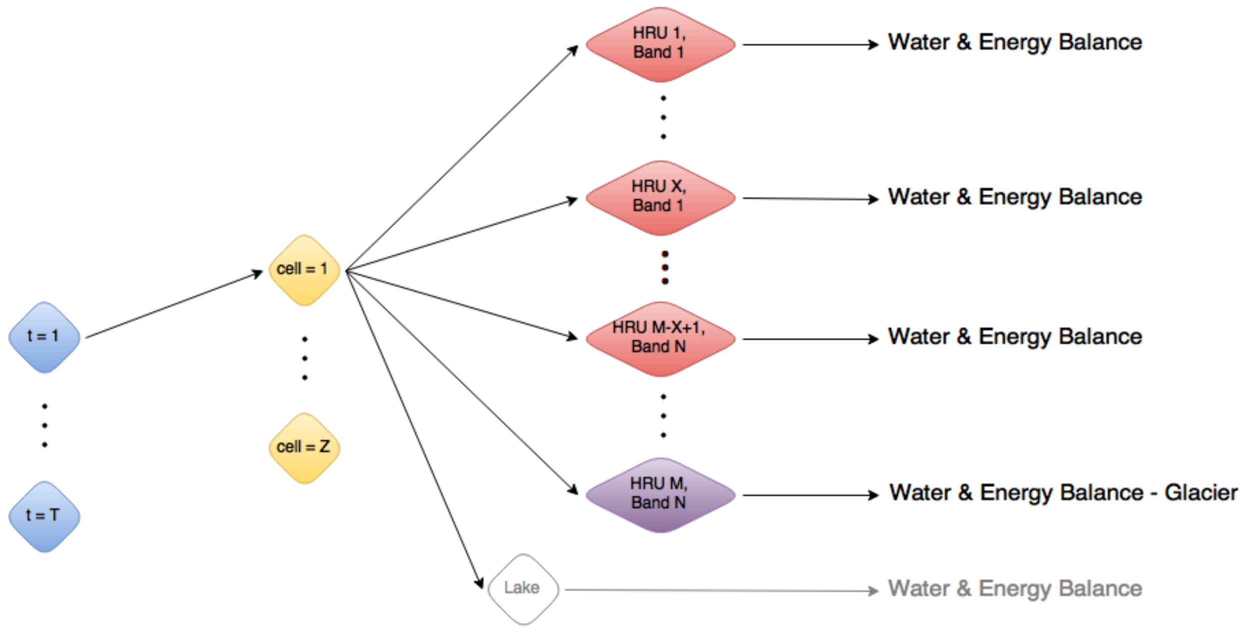

Figure 6. Order of operations for glacier version of VIC. Note that the treatment of lakes is currently an untested code path in the VIC-GL model.

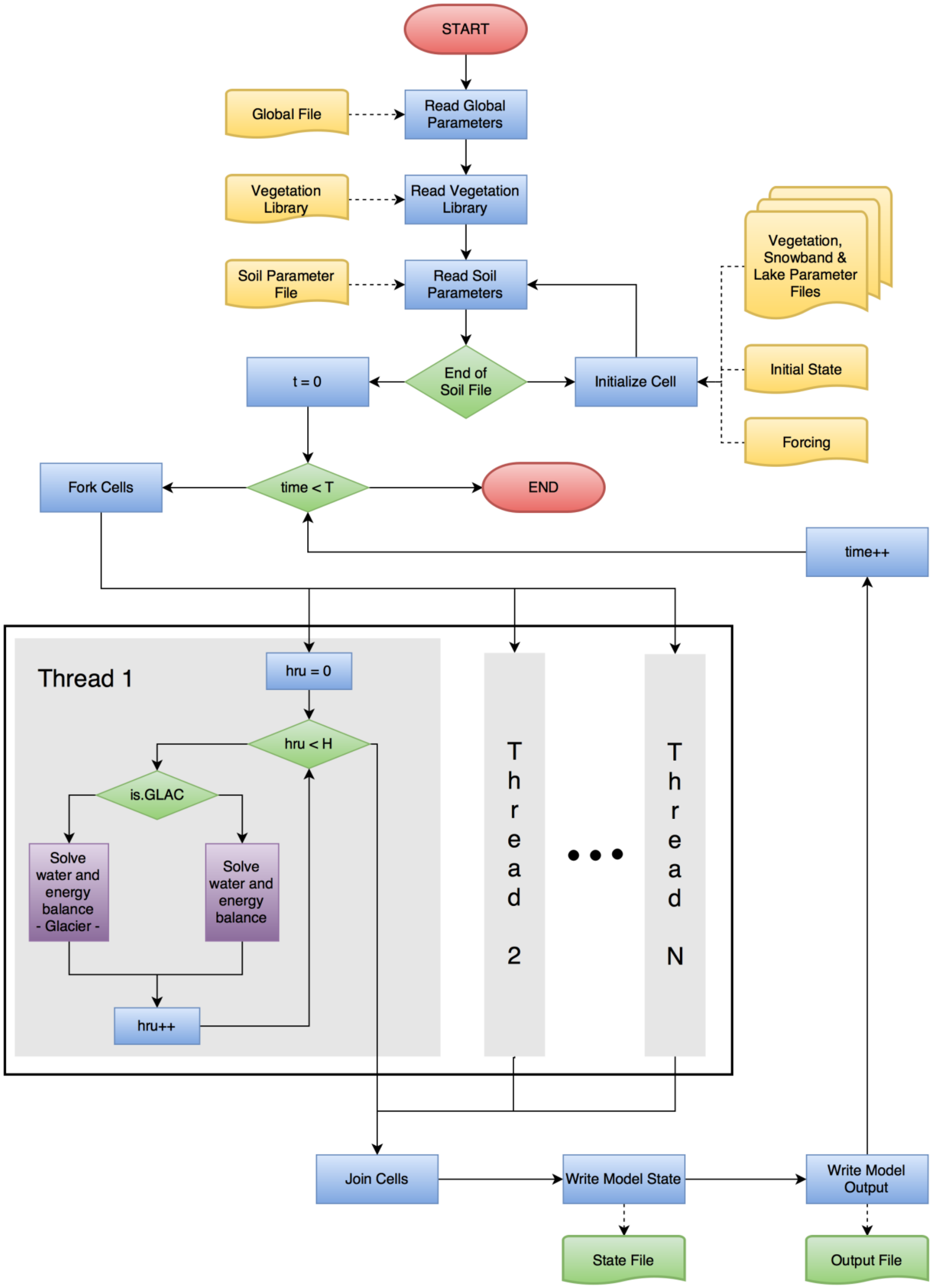

Figure 7. VIC-GL main program flow with time-major looping, multi-threaded cell processing and HRU vectorization.

2.5 I/O

The original version of VIC read model forcing and wrote model output using flat files (in either ASCII or binary format) for each grid. This resulted in multiple files for each grid cell, which made inefficient use of file systems, particularly when large domains can include > 10^4 grid cells. This also made for an awkward storage format for multi-dimensional (3D or 4D) data. Users now have the option of writing output in the much more efficient self-describing netCDF format, which allows multi-dimensional output to be efficiently stored in a single file. The use of ASCII output is still available (although discouraged) and binary output option no longer available. NetCDF format option is available for model input, output, and state. The use of netCDF I/O is implemented using the settings given in Table 3.

Table 3. Parameter settings for netCDF file I/O.

Location	Parameter	Value
user_def.h	NETCDF_OUTPUT_AVAILABLE	TRUE
Global file	OUTPUT_FORMAT	NETCDF
Global file	STATE_FORMAT	NETCDF
Global file	COMPRESS	If TRUE, will compress netCDF output using built-in compression for netCDF 4. Compression level is hard coded at level 1 (options range from 0 (no compression) and 9 (maximum compression).
Global file	NETCDF_OUTPUT_FILENAME	Name of netCDF output file. If not explicitly set, default is result.nc
Global file	NETCDF_ATTRIBUTE	Set global attribute for netCDF file. Specify both netCDF attribute name (e.g.,’ title’) and attribute value (i.e. accompanying text).

2.6 Additional Features

2.6.1 Memory Check

With the change to time-major looping (i.e., model now runs in image mode) a check has been added to ensure that all the model cells will fit in system memory. If a maximum memory is specified (see MAX_MEMORY setting in Table 4) then the model will return a warning if the estimated RAM required exceeds this limit.

2.6.2 Precipitation Partitioning

The original VIC formulation assumes a linear relationship with temperature where mixed precipitation occurs between a maximum temperature for snow occurrence and a minimum temperature for rain occurrence (both specified as parameters by the user). However, a review of the literature suggests that a curvilinear approach is the most accurate means of describing the frequency of rain (or snow) occurrence. Hence, VIC has been updated to use the more realistic precipitation partitioning algorithm of Kienzle (2008). The chosen method is based on two parameters, the threshold mean daily temperature (T_T), where 50% snowfall occurs, and the range of temperatures (T_R) within which both solid and liquid precipitation occurs. This means that the curve can be both stretched along the x-axis by increasing the T_R variable and moved along the x-axis by changing the T_T variable, according to observations or calibration at a specific location. The calculation of rainfall proportion is

$$P_{rain} = \begin{cases} 0 & for\ T \leq T_T - T_R/2 \\ 5E^3 + 6.67E^2 + 3.19E + 0.5 & for\ T \leq T_T \\ 5E^3 - 6.67E^2 + 3.19E + 0.5 & for\ T \geq T_T \\ 1 & for\ T \geq T_T + T_R/2 \end{cases} \tag{5}$$

where E is

$$E = \frac{T - T_T}{1.4 \cdot T_R}. \tag{6}$$

The user now has a choice between the new Kienzle algorithm or the original VIC algorithm (see TEMP_TH_TYPE setting in Table 4).

Table 4. Parameter Settings for Additional Features (memory checking and precipitation partitioning)

Location	Parameter	Value
Global file	MAX_MEMORY	System memory limit in Gigabytes. A setting of 0.0 (default) indicates that unlimited memory is assumed.
Global file	TEMP_TH_TYPE	KIENZLE = algorithm of Kienzle (2008) (default); VIC_412 = original VIC algorithm

2.7 Code Paths and Modes of Operation

Only the following operational modes have been tested and verified (valid using both TRUE and FALSE settings in the global file)

- Output Force (OUTPUT_FORCE = TRUE)
- Water Balance mode (FULL_ENERGY = FALSE)
- Energy balance mode (FULL_ENERGY = TRUE; QUICK_FLUX = TRUE)

Several model options and code paths remain untested for compatibility with the new glacier upgrades. In other words, these options have only been validated for the default FALSE setting in the global file (Table 5) or the FALSE definition in the user_def.h file (

Table 6).

Table 5. Untested Model Options Set from the Global File

Process	Parameter	Description
Distributed precipitation	DIST_PREC	If TRUE use distributed precipitation. This feature is deprecated.
Handling the water/ice phase change in frozen soils	FROZEN_SOIL	If TRUE, account for water/ice phase change (including latent heat). If FALSE, soil moisture always remains liquid, even when below 0 C, with no latent heat effects and ice content is always 0.
Solution to soil heat flux equation	IMPLICIT	If TRUE the model will use an implicit solution for the soil heat flux equation, (QUICK_FLUX is FALSE), otherwise uses original explicit solution.
Hybrid option for converting vertical soil temperature profile	QUICK_SOLVE	If TRUE model will use the method described by Liang et al. (1999) to compute ground heat flux during the surface energy balance iterations, and then will use the method described in Cherkauer and Lettenmaier (1999) for the final solution step.
Type of soil bottom boundary	NO_FLUX	If TRUE model will use a no flux bottom boundary with the finite difference soil thermal solution (i.e., QUICK_FLUX = FALSE or FULL_ENERGY = TRUE or FROZEN_SOIL = TRUE). Default = FALSE (i.e., use a constant temperature bottom boundary condition).
Vertical distribution of soil thermal nodes	EXP_TRANS	If TRUE the model will exponentially distribute the thermal nodes in the Cherkauer and Lettenmaier (1999) finite difference algorithm, otherwise uses linear distribution. (This is only used if FROZEN_SOIL = TRUE).
Lakes	LAKES	If FALSE do not simulate lakes; if TRUE simulate lakes using the dynamic lakes/wetlands model and read the given lake parameter file for lake model parameters.
Blowing Snow	BLOWING	If TRUE, compute evaporative fluxes due to blowing snow.
Compute Treeline	COMPUTE_TREELINE	This option is deprecated with the introduction of HRUs.

Table 6. Untested Code Paths Defined in the user_def.h File

Process	Parameter	Description
Quick Frozen Soil	QUICK_FS	If TRUE VIC uses a system of linear equations to estimate the maximum unfrozen water content equation
Excess Ice	EXCESS_ICE	If TRUE VIC uses a uniform distribution function to simulate the spatial distribution of soil frost; if FALSE VIC assumes that the entire grid cell is frozen uniformly.
Spatial Frost	SPATIAL_FROST	If TRUE VIC uses a uniform distribution to simulate the spatial distribution of soil frost; if FALSE VIC assumes that the entire grid cell is frozen uniformly
Spatial Snow	SPATIAL_SNOW	If TRUE VIC uses a uniform distribution to simulate the partial coverage of the surface by a thin snowpack. Coverage is assumed to be uniform after snowfall until the pack begins to melt
Close energy balance	CLOSE_ENERGY	If TRUE, all energy balance calculations are iterated to minimize the total column (air, canopy, snow, and ground) error. Otherwise, no iteration is used, and the model estimates the new fluxes based on those from the previous time step.
Low resolution moisture	LOW_RES_MOIST	If TRUE, VIC uses the linear interpolation of the logarithm of the matric potential from the two surrounding layers to estimate the soil moisture drainage from each layer.

3 Glacier Processes

3.1 Glacier Mass and Energy Balance

Glacier mass balance modelling is the 1-dimensional (i.e., vertical) simulation of glacier ice accumulation and melt (including any seasonal snow accumulation and melt). This capability is necessary for short-term hydrologic modelling (e.g., seasonal, and annual forecasting or decadal prediction) in glacierized basins. In addition, glacier net mass balance is the required forcing for the glacier dynamics model (§**Error! Reference source not found.**). As stated previously, the occurrence of glaciers requires a separate glaciers land cover class, which spawns the creation of glacier HRUs in those elevation bands that contain glaciated terrain. The simulation of the 1-dimnesional mass and energy balance for glaciers uses a separate code path for glacier HRUs. This includes the necessary routines/algorithms to model mass and energy balance of glacier ice within glacier HRUs as well as melt water storage and routing.

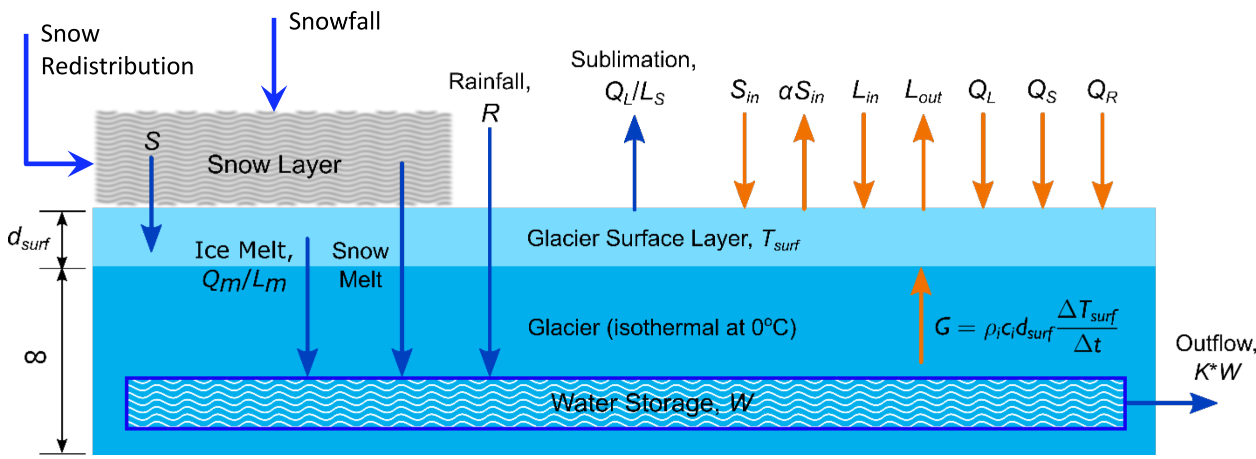

Figure 8. Schematic of the glacier mass and energy balance model, showing mass (blue arrows) and energy (orange arrows) fluxes modelled by VIC-GL. Note that the snow and glacier energy balance are treated independently, where snow accumulation and melt are modelled using VIC's original algorithm.

3.1.1 Glacier Ice Mass Balance

For integration with existing VIC routines, glacier mass balance refers specifically to the mass balance of glacier ice and does not include surface snow. The mass balance of snow on the surface of a glacier is simulated within the existing VIC snow mass balance model (Andreadis et al. 2009). The glacier energy balance model incorporates the existing input or forcing data as that for the existing snow surface energy balance model.

The 1-dimensional (i.e., vertical) glacier net mass balance, *M* (m of water equivalent), is evaluated as the integral of the specific balance rate, $m(x, t)$ over a time interval t_1 to t_2

$$M = \int_{t_1}^{t_2} m(x,t)\,dt \tag{7}$$

where $m(x, t)$ (units of m/s) is the water equivalent rate of ice melt, ice sublimation and ice accumulation (via the conversion of snow/firn to glacier ice) at some point *x* on the glacier surface. Hence, glacier net mass balance can be stated as (Klok and Oerlemans 2002)

$$M = \int_{t_1}^{t_2} \left(\frac{H_m}{\rho_w L_m} + \frac{H_l}{\rho_w L_s} + S\right) dt \tag{8}$$

where H_m and H_l are the energy involved in melting and sublimation, respectively (units of W m^{-2}), L_m is the latent heat of melting (3.34 x 10^5 J kg^{-1}) and L_s is the latent heat of sublimation (2.83 x 10^6 J kg^{-1}), ρ_w is the density of water (999.84 kg m^{-3} at 0°C), and S is water equivalent ice accumulation (m/s) (from conversion of snow/firn to ice). See Section 3.1.2 for discussion of the energy balance terms H_m and H_l.

The model treats snow and firn (compacted snow left over from the previous season) as a combined snowpack and modelled using the existing VIC snow mass balance model; there is no explicit distinction between snow and firn. The most physically based approach to convert firn to ice (i.e., to remove mass from the snowpack and add it to the glacier) would be to use the modelled snowpack density, i.e., firn becomes glacier ice when the snowpack density exceeds the close-off density[1] of 830 kg m^{-3}. Then S in equation (8) is the amount of firn with density greater than the given threshold at the end of the desired integration period (monthly or annual, to be determined). VIC does not calculate density of the snowpack explicitly, but does calculate the mass in snow water equivalent, *swe*, and depth, z_{snow}, of the snowpack. Hence, the average (or bulk) snow/firn density is calculated as

$$\overline{\rho_s} = \frac{swe}{z_{snow}}\,\rho_w \quad . \tag{9}$$

Snow/firn density increases with depth (Cuffey and Paterson 2010) and for simplicity we assume a linear profile from value of ρ_o = 350 kg/m^3 at the snow surface (Herron and Langway 1980) to $\overline{\rho_s}$ at a depth of $z_{snow}/2$. Hence, the variation of snow/firn density with depth, z is

$$\rho(z) = \begin{cases} \overline{\rho_s}, & \overline{\rho_s} \le 350 \\ \rho_o + \left(\dfrac{\overline{\rho_s} - \rho_o}{z_{snow}/2}\right) z, & \overline{\rho_s} > 350 \end{cases} \tag{10}$$

[1] At a density of 830 kg m^{-3} all air passages between ice crystals are sealed off; this defines the transition from firn to ice (Cuffey and Paterson 2010)

where, for a shallow snowpack when $\overline{\rho_s}$ is less than or equal to 350 kg/m^3, $\rho(z)$ is set equal to $\overline{\rho_s}$. The depth to the close-off density, z_{co}, is calculated by solving equation (4) for z at ρ = 830 kg/m^{-3} when $\overline{\rho_s} > 350$. Effectively, z_{co} only exceeds z_{snow} when $0 < (\rho(z) - \rho_0)/2(\overline{\rho_s} - \rho_0) < 1$. Estimation of the conversion of snow to fern S (as water equivalent depth) uses

$$S = \begin{cases} 0, & z_{co} \geq z_{snow} \; or \; \overline{\rho_s} \leq 350 \\ \dfrac{[\rho(z_{snow}) + \rho(z_{co})]}{2\rho_w}(z_{snow} - z_{co}), & z_{co} < z_{snow} \end{cases} \quad . \tag{11}$$

The updated snow water equivalent of remaining snow/firn is simply $swe - S$, the updated snow/firn depth is z_{co}, and the updated average (or bulk) snow/firn density is

$$\overline{\rho_s}' = \frac{(swe - S)\rho_w}{z_{co}} \quad . \tag{12}$$

Estimation of S is the mechanism by which VIC snow and glacier mass balances are directly coupled.

3.1.2 Glacier Surface Energy Balance

For convenient integration with VIC, the snow surface and ice surface energy balances have separate treatments. The existing VIC implementation is used for calculating the snowpack energy balance, which treats snow and firn as one combined “snowpack”; we assume a continuous transition from snow to firn when seasonal snow disappears (e.g., old seasonal snow has same albedo as newly exposed firn, etc.).

For bare glacier ice, i.e. when no snow is present, the vertical energy Flux, F, at the glacier surface is modeled as (Klok and Oerlemans 2002)

$$F = R_{in} + R_{out} + L_{in} + L_{out} + H_h + H_l = H_m + G \tag{13}$$

where R_{in} and R_{out} are incoming and reflected solar radiation, L_{in} and L_{out} are incoming and emitted longwave radiation, H_h and H_l are the sensible and latent heat fluxes. All fluxes on the left side of equation (13) are positive towards the surface. The surface energy flux provides energy for melting (H_m) and for the glacier heat flux (G), which implies the warming (cooling) of the ice surface due to conduction of heat to (from) the surface from (to) the glacier mass. Calculation of R_{in}, R_{out}, L_{in}, L_{out}, H_h and H_l uses the existing routines in VIC, with appropriate adjustments made to glacier parameters controlling surface roughness, albedo, and emissivity of glacier ice. Modification of solar and longwave radiation due to slope, aspect and topographic shading is ignored.

3.1.3 Glacier Heat Flux and Surface Temperature

The energy balance with respect to calculating ice temperature within the glacier assumes a temperate glacier with a seasonally varying thin cold surface layer (Paterson 1994). In this case, heat flow (heat diffusion) is the dominant mechanism in the surface layer and internal heat generation (e.g. heat release due to ice deformation, sliding friction, refreezing of melt water), geothermal heat, and advection is neglected (Paterson 1994). Heat flux between the base of glacier and the ground is assumed zero (i.e., both glacier base and ground are at the temperature of the pressure melting point of ice). The glacier heat flux, G, and resultant changes in surface temperature, T_s, are solved iteratively following Wheler and Flowers (2011). When the glacier is bare (i.e., no snow or firn layer), and when the glacier surface temperature is less than zero or F is negative, melt energy is zero and glacier flux is equal to the surface energy flux (i.e., G is the residual of the energy balance equation). The resultant changes in surface temperature, and related changes in the turbulent fluxes and the surface energy balance are then recomputed. For each timestep, the energy balance is calculated initially with T_s = 0°C and G is taken as the residual of equation (13). The temperature change in the surface layer is then calculated from G as the change in cold content (Wheler and Flowers 2011)

$$\Delta T_s = \frac{G}{\rho_i\, c_i d_s}\Delta t \tag{14}$$

where ρ_i is the density of ice (917 kg m^{-3} at 0°C), c_i is the specific heat capacity of ice (2100.0 J kg^{-3} C^{-1}) and d_s is the thickness of the surface layer (set by the user) and Δt is the timestep, in seconds. The surface energy balance is re-calculated with the new T_s, and the iteration continues until T_s stabilizes (i.e., incremental change in T_s converges to ±0.25 °C).

3.1.4 Melt Flux

Melting occurs when the surface temperature is at the melting point (T_s = 0°C) and the surface energy flux is positive. In such a case, the glacier heat flux is zero and $H_m = F$. Melting can also occur if the surface temperature is below freezing but the surface energy flux, F, is positive and larger than the surface layer cold content ($F > -\rho_i c_i T_s d_s$). In this case T_s is set to 0°C and H_m is calculated as

$$H_m = F - \rho_i c_i \frac{\Delta T_s}{\Delta t} d_s \tag{15}$$

3.1.5 Surface Energy Balance – With Snow/Firn

When the glacier is covered in snow/firn, equation (15) reduces to $F = G$, where $G_{ice} = -G_{snow}$, and G_{snow} is calculated from the VIC snow pack energy balance as (Cherkauer and Lettenmaier 1999)

$$\kappa_{snow}\frac{\Delta T_{snow}}{z_{snow}} = G = -\kappa_i \left.\frac{dT}{dz}\right|_{z=0} \tag{16}$$

where κ_{snow} is the thermal conductivity of snow[2], ΔT_{snow} is the change in temperature from the snow surface to the ice surface (C), κ_i is the thermal conductivity of ice (currently set as 2.2 W m^{-1} K^{-1} in VIC), and z_{snow} is the depth of the snowpack (m). The temperature of the surface layer is then calculated, as per §3.1.3, as part of the existing snowpack energy balance.

3.1.6 Transfer of Cold Content in S

The conversion of snow/firn mass to glacier ice mass as *S* in equation (8) also implies the transfer of cold content between the two mediums. The temperature of converted snow/firn assumes a linear temperature profile through the snow/firn pack layer, as per (18), such that the bulk temperature of *S* is

$$T_S = T_{snow}^0 + \left(\frac{\Delta T_{snow}}{z_{snow}}\right)\left(\frac{z_{snow} + z_{co}}{2}\right) \quad (17)$$

where T_{snow}^0 is the temperature of the snow surface. The cold content contained in the mass of converted snow/firn, *S*, is then given as

$$CC_S = -\left[\frac{\rho(z_{snow}) - \rho(z_{co})}{2}\right] c_i T_S \left(z_{snow} - z_{co}\right) \quad (18)$$

where $\rho(\cdot)$ is calculated using (10). The updated cold content of the glacier ice surface is $CC_{ice}' = CC_{ice} + CC_S$, such that the updated glacier surface temperature is calculated as

$$T_S' = \frac{CC_{ice}'}{\rho_i c_i d_s} = T_s + \frac{CC_S}{\rho_i c_i d_s} \quad (19)$$

where is it assumed that the cold content is only added to the thin surface layer, d_s. The change in cold content in the remaining snow/firn layer is simply $-CC_S$ such that the change in snow/firn temperature is

$$T_{snow}' = \frac{CC_{snow} - CC_S}{\bar{\rho}_s{}' c_s \, z_{snow}{}'} \quad (20)$$

where z_{snow}' is equal to z_{co}.

3.1.7 Snow Redistribution

Redistribution of snow, by either wind or avalanche, can be important in determining the presence of glaciers and in controlling glacier mass balance (Dadic et al. 2010; Elder 1995; Grabiec et al. 2011). It is

[2] Thermal conductivity of snow is currently calculated in VIC as a function of snow density using 2.9302 x 10^{-6} ρ_s^2 (reference unknown)

the purpose of this update, therefore, to incorporate snow redistribution between non-glaciated and glaciated terrain to simulate more plausible mass balance quantities and sub-grid snow variability.

The proposed method is in some ways similar to that suggested by Kuhn (2003) in that snow redistribution is implemented indirectly via changes in the magnitude of snowfall between glaciated and non-glaciated areas. Nevertheless, the approach advocated by Kuhn (2003) is overly simple as it assumes that the volume of solid precipitation in glacier areas is doubled (i.e. glaciers receive twice as much precipitation as the basin average) and volume of precipitation in non-glaciated terrain is simply the residual of the total volume. This approach does not automatically conserve precipitation volume per band (i.e., precipitation in non-glaciated terrain can be negative if the glacier area is over 50% of band area).

We propose a modification to this approach wherein the change in precipitation for glaciers is proportional to glacier area in an elevation band. In other words, the volume of snow redistribution is assumed to be controlled be the size of the boundary between glaciers and the surrounding terrain. If a glacier is relatively small, then only a small proportion of the surrounding terrain contributes additional snow; likewise, if the glacier is relatively large then more of the surrounding terrain will contribute additional snow. The precipitation rate in non-glaciated terrain (which is assumed to be losing snow) is given as

$$P_{ng}[b,t] = P[b,t](1 - G[b]) \tag{21}$$

where

$$G[b] = \frac{A_g[b]}{A[b]} R \tag{22}$$

where A_g and A are the glacier and total area for band b, respectively, P is the band-average precipitation rate at time t, and R is a scaling factor ranging from 0 (no redistribution; G=0) to 1 (redistribution scales equivalently with proportion of glacier area). By ensuring conservation of mass, the precipitation rate for glaciers is then

$$P_g[b,t] = \frac{P[b,t]A[b] - P_{ng}[b,t]A_{ng}[b]}{A_g[b]} = P[b,t]\frac{\{A[b] - (1 - G[b])A_{ng}[b]\}}{A_g[b]}. \tag{23}$$

Equations (22) and (23) ensure conservation of mass, so long as $R \le 1.0$. When R=0, then $P_g[b,t] = P_{ng}[b,t] = P[b,t]$. Equation (23) is undefined when A_g=0, however, in the limit as $A_g[b] \to 0, P_g[b,t] \to P[b,t]\{1 + R\}$; conversely as $A_{ng}[b] \to 0, P_{ng}[b,t] \to P[b,t]\{1 - R\}$ (see Figure 9).

A practical example of the nature of the redistribution algorithm is provided using the Peyto glacier VICGL application. The area-elevation of Peyto glacier is given in Figure 10, wherein we see that the overall area distribution peaks at about 2600 m elevation. The ratio of glacier area to band area also peaks at 2600 m elevation, decreasing to zero (i.e., glacier area is zero) with increasing and decreasing elevation.

3.1.8 Discussion of Limitations

The relevant features and limitations of the mass and energy balance model include:

- Glaciers are modeled as two layers: a thin surface layer of varying temperature with an underlying isothermal ice layer at a constant 0°C temperature. Energy exchange occurs only with the thin surface layer.
- Heat from other sources, e.g., basal friction, internal deformation, phase changes, and geothermal heat flux, is ignored. Heat conduction between snow and ice is also ignored.
- The underlying ice layer is of infinite thickness (modelling of glacier volume and area changes are the subject of the glacier dynamics component).
- The model does not consider the effects of slope, aspect, terrain shading or debris on incoming radiation or snow re-distribution by wind and gravity.
- For simplicity snow redistribution does not consider wind fields and other topographic factors that directly control snow redistribution (e.g. Carturan et al. 2009; Gruber 2007) and it assumes that snow is only distributed from non-glaciated to glaciated terrain (the model does not consider snow redistribution between non-glaciated terrain elements, i.e. snow avalanches into forested terrain). The model only applies to existing glaciers (i.e., a glacier HRU must be present in elevation band) and would not affect glacier seeding or initiation. However, this is not considered a serious issue in the context of future climate simulations where glaciers are expected to shrink (although it may, perhaps, have an indirect effect during model spin-up).

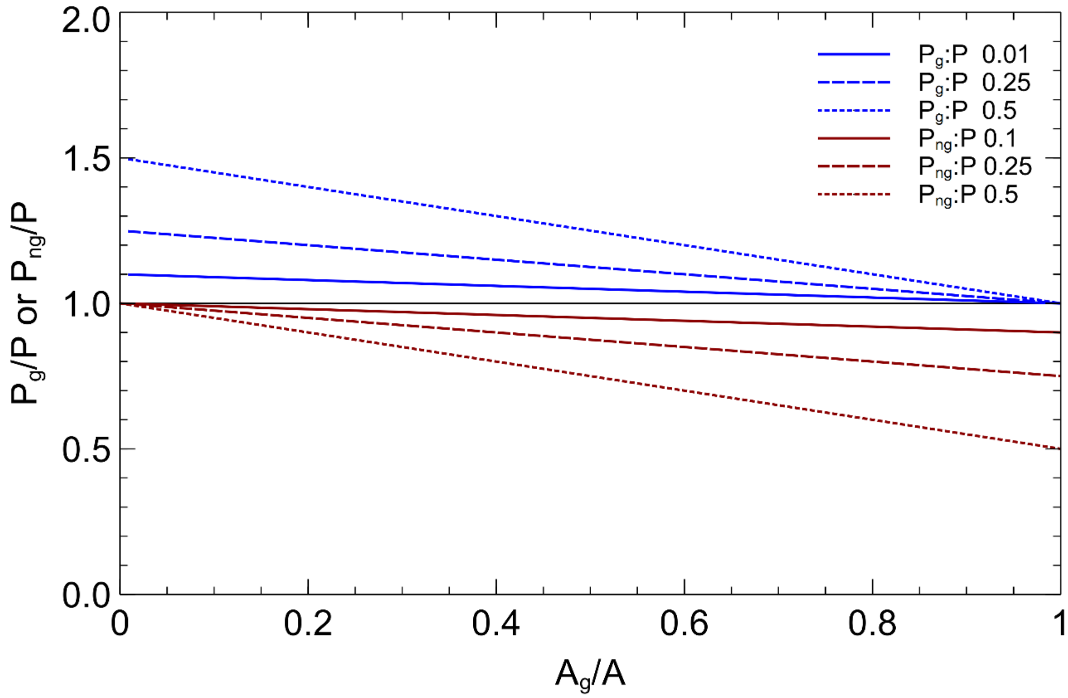

Figure 9. Change in glacier and non-glacier precipitation (as a proportion of total precipitation) as a function of proportional glacier area for R equal to 0.1, 0.25 and 0.5.

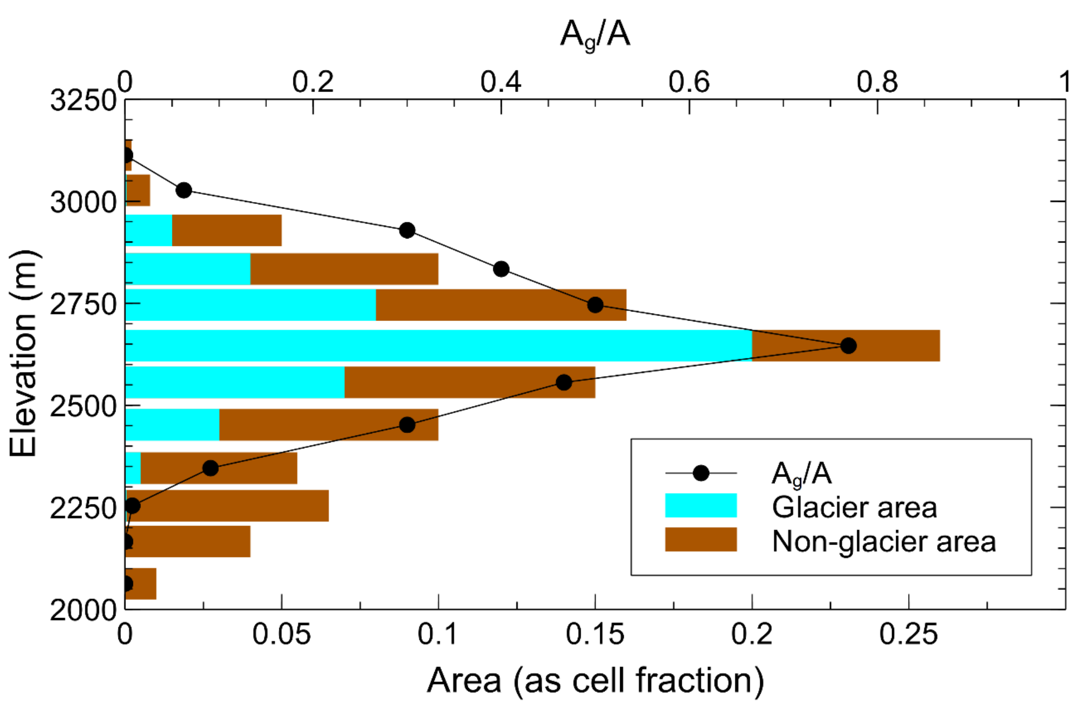

Figure 10. Peyto glacier area-elevation distribution based on 100-m elevation bands.

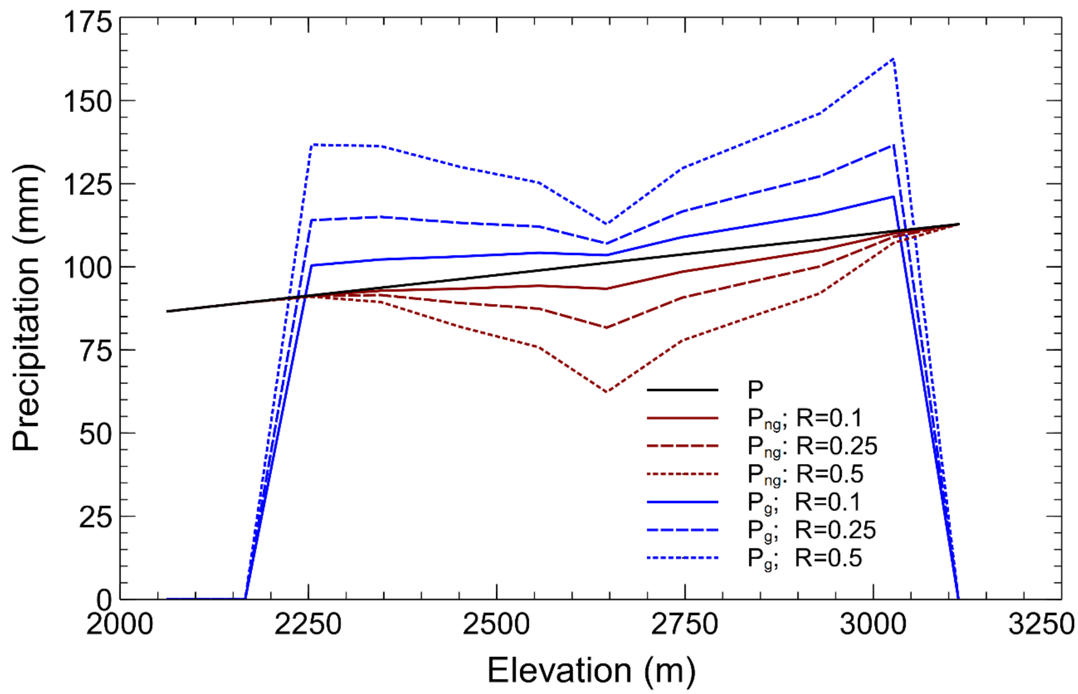

Figure 11. Precipitation gradients when using snow redistribution.

3.1.9 Mass Balance Sensitivity

The mass balance sensitivity was tested against variation of 11 model parameters (which are summarized in Table 7). The parameter ranges given in Table 7 were sampled using the Sobol quasi-random sampling (SRS), conducted using the R `sensitivity::sobolSalt` function (in 'offline' mode) in the R `sensitivity` package (Iooss et al. 2019). VICGL simulations used 50 samples (X1 and X2) for a total of $n(2p+2) = 1200$ model evaluations (where n is the sample size and p is the number of parameters). The root-mean-square error of the winter, summer, and annual surface mass balance (by elevation) provided the metrics for assessing model sensitivity. Sensitivity was measured using Sobol first-order, second-order and total effects indices based on Saltelli schemes (using R function `sensitivity::sobolSalt`) (Saltelli 2002). Sensitivity was assessed separately for the winter (1 Oct, previous year to 31 March, current year), summer (1 Apr to 30 Sep, current year) and net (winter-summer) mass balance periods during the period 1/1/1960 to 31/12/1995. Sensitivity was assessed for four different locations modelled on the Bridge, Peyto, Place and Tiedemann glaciers.

Based on the 'total-effects' indices (Figure 12), winter mass balance shows highest sensitivity to *padj.s, pgrad* and *rdef*, three parameters that control snowfall deposition on the glaciated terrain. Between all four sites, summer mass balance is sensitive to the total effects of *ns.alb*, *padj.s*, *tlapse*, *tth1*, *tth2* and *g.alb*, indicating the importance of snow cover duration and solar radiation upon the summer mass balance (Figure 12). The model shows very little sensitivity to *g.thick*, *g.rough* or *padj.r* (Figure 12).

Table 7. Parameters and ranges used to assess VIC-GL mass balance sensitivity

Parameter	Description	Range	Units
ns.alb	Albedo of new snow	0.75 - 0.95	--
tth1	Temperature threshold parameter – median	-1.0 - 5.0	°C
tth2	Temperature threshold parameter – range	5.0 - 20	°C
padj.r	Precipitation scaling factor for rainfall	0.5 - 2.0	--
padj.s	Precipitation scaling factor for snowfall	0.5 - 2.0	--
tlapse	Temperature lapse rate	0.2 - 10	°C km^{-1}
pgrad	Precipitation change factor with elevation	0.010 - 0.075	100 m^{-1}
g.thick	Glacier surface thickness	10.0 - 200	mm
g.alb	Glacier albedo	0.2 - 0.6	--
g.rough	Glacier surface roughness	0.0001 - 0.0100	m
rdef	Glacier snow redistribution factor	0.0 - 1.0	--

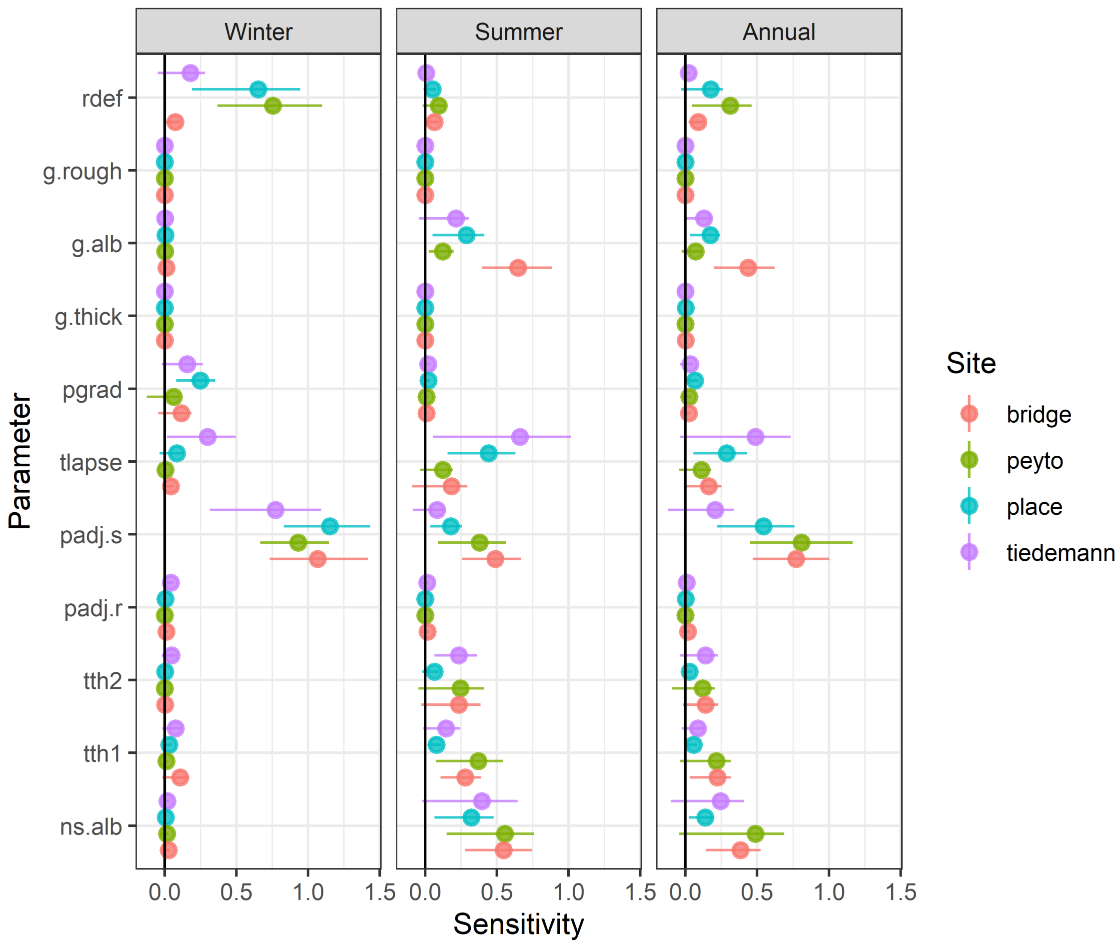

Figure 12. Sobol 'Total effects' sensitivity indices of winter, summer and net annual glacier-average surface mass balance as a function of model parameters. Ranges show 95% confidence interval.

3.2 Glacier Water Storage

This section describes the modelling of sub-, en- and supra-glacial storage, routing, and movement of runoff from snow melt, glacier melt and rainfall within glacier ice in each glacier HRU. Note that storage and percolation of rainfall and melt water in the snowpack is handled separately by the existing VIC model.

All runoff generated within a glacier HRU, whether from snowmelt (technically percolation of water out the base of the snowpack), glacier melt (calculated from equation (9)) or rainfall, is assumed to occur on the glacier surface and enter and move through either the supra-, en- or sub-glacial drainage networks. Water infiltration in the till, sediment or bedrock below the glacier is ignored. Glacier outflow is modelled using a storage discharge relation of the form (Stahl et al. 2008)

$$Q_g(t) = K(t) \cdot W(t) \tag{24}$$

where $W(t)$ is the liquid water in supra-, en- and sub-glacial storage at time t (mm) and $K(t)$ is a time-varying outflow coefficient parameterized as a function of snow water equivalent as

$$K(t) = K_{min} + dK \cdot \mathrm{e}^{-\mathrm{A}\cdot\mathrm{swe(t)}} \tag{25}$$

where K_{min} is the minimum outflow coefficient value, representing conditions with deep snow and poorly developed supra-, en- and sub-glacial drainage networks (time^{-1}) (typical of mid-winter or early spring conditions), $K_{min} + dK$ is the maximum outflow coefficient, representing well developed glacial drainage conditions under bare ice (typical of late summer in the ablation zone), A is a calibration parameter (mm^{-1}), and $swe(t)$ is the snow/firn water equivalent for time t (mm). Figure 13 shows the sensitivity of the glacier outflow coefficient to the value of parameter A. Note that W(t) in (25) is unconstrained (e.g., currently no upper limit is specified as, say, a function of glacier depth). All glacier outflow, $Q_g(t)$, is added to the surface drainage network as part of surface runoff.

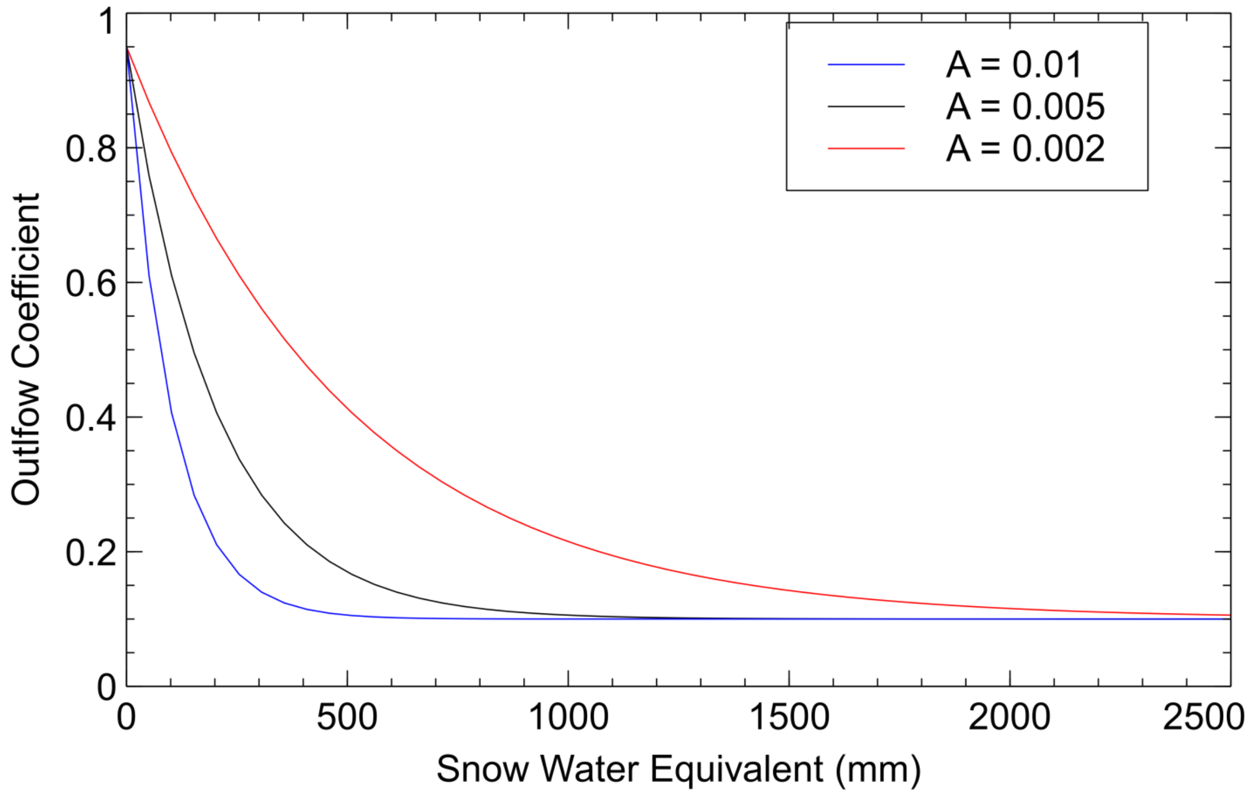

Figure 13. Relationship between outflow coefficient, *K*, and snow water equivalent, *swe*, for various values of *A*. Function plotted using K_{min} = 0.1 and *dK* = 0.85.

3.3 Glacier Dynamics

The VIC-GL model is not designed to allow lateral communication between cells; hence, it can't be used to directly model hydrologic or cryospheric features that occupy more than a single cell (such as large lakes or ice fields), or that flow from one cell into another cell (such as valley glaciers). Consequently, glacier dynamics is simulated by coupling VIC-GL to the UBC Regional Glaciation Model (RGM). The RGM model is described in detail by Jarosch et al. (2013) and Clarke et al. (2015). The coupled modelling system, which is run using the Hydro-Conductor wrapper, is discussed in a separate document (Schnorbus 2018).

Although glacier dynamics is not modelled explicitly in VIC-GL, running the model as part of the coupled system requires calculation and output of the surface mass balance elevation gradient on an annual, or multi-annual, basis. The gradient is modelled using a quadratic equation fit to the cumulative annual (or multi-annual) band-average surface mass balance (predictor) and the band median elevation (predictand). The integration period for calculating the balance gradient is defined by the user as part of the model parametrization (see §3.4). The gradient is calculated at the end of the integration period and the fitted model coefficients are stored in the VIC state file (as opposed to the normal output file).

Table 8. New Variables for Glacier Mass and Energy Balance Modelling

Variable	Description	Units	Output†	Scope‡
Water Balance State				
W	Glacier water storage	m	O/S	B/C
A_g	Glacier surface area (as cell area fraction)	fraction	O/S	B/C
Water Balance Fluxes				
M	Total glacier net mass balance	mm/timestep	O/S	B/C
I	Glacier ice net mass balance	mm/timestep	O/-	B/C
S	Ice accumulation from conversion of snow/firn	mm/timestep	O/-	B/C
$H_m/\rho_w L_m$	Ice melt	mm/timestep	O/-	B/C
$H_l/\rho_w L_s$	Ice sublimation/condensation	mm/timestep	O/-	B/C
$H_m/\rho_w L_m + O_{snow} + R$	Glacier water inflow from snowpack outflow, ice melt and rainfall	mm/timestep	O/-	B/C
Q_g	Glacier outflow/discharge	mm/timestep	O/-	B/C
Water Balance Miscellaneous				
K	Glacier outflow coefficient	fraction	O/-	-/C
Energy Balance State				
T_s	Glacier surface temperature	°C	O/S	B/C
Energy Balance Fluxes				
$-\rho_i c_i \frac{\Delta T_s}{\Delta t} d_s$	Change of cold content in glacier surface layer	W m^{-2}	O/-	-/C
G	Energy flux through glacier surface layer	W m^{-2}	O/-	-/C
H_m	Energy used to thaw glacier ice	W m^{-2}	O/-	-/C
Mass Balance Gradient Model Terms				
Terms	b_0 b_1 b_2 fit error	m m/m m/m^2 m	-/S	-/C

† O is written to output file; S is written to state file

‡ B is available as band-average average; C is available as cell-average

3.4 New Parameters and Constants

The upgrading of the VIC model to incorporate both glacier mass-energy balance and accommodate dynamics modelling has resulted in the addition of several new model parameters, output variables and model configuration settings. The new output and state variables are summarized in Table 8. Of the new parameters, summarized in Table 9, most have been introduced via addition to the soil parameter file; ice emissivity has been added as a global parameter. New model configuration settings, which are set in the global file, are summarized in Table 10.

Table 9. New Parameters for Glacier Mass and Energy Balance Modelling

Symbol	Name	Location
d_s	Thickness of glacier surface layer	Soil Parameter File
K_{min}	Minimum glacier outflow coefficient	Soil Parameter File
dK	$K_{min} + dK$ is maximum outflow coefficient	Soil Parameter File
A	Calibration parameter	Soil Parameter File
α_g	Glacier surface albedo	Soil Parameter File
ε_g	Emissivity of glacier ice	vicNl_def.h
z_o	Ice surface roughness	Soil Parameter File
R	Scaling factor for snow redistribution	Soil Parameter File

Table 10. New Global File Parameters for Glacier Mass and Energy Balance Modelling

Parameter	Description
GLACIER_ID	ID of glacier class in the vegetation library
GLACIER_ACCUM_START_YEAR	Year on which to begin tracking cumulative mass balance
GLACIER_ACCUM_START_MONTH	Month on which to begin tracking cumulative mass balance
GLACIER_ACCUM_START_DAY	Day on which to begin tracking cumulative mass balance
GLACIER_ACCUM_INTERVAL	Interval (in years) over which to track glacier mass balance – effectively the temporal frequency of the dynamics model
OPEN_ID	ID for open class in the vegetation library

4 References

Andreadis, K. M., P. Storck, and D. P. Lettenmaier, 2009: Modeling snow accumulation and ablation processes in forested environments. *Water Resour. Res.*, **45**, https://doi.org/10.1029/2008WR007042.

Barry, R. G., 1992: *Mountain weather and climate*. Routledge, 402 pp.

Carturan, L., F. Cazorzi, and G. Dalla Fontana, 2009: Enhanced estimation of glacier mass balance in unsampled areas by means of topographic data. *Ann. Glaciol.*, **50**, 37–46, https://doi.org/10.3189/172756409787769519.

Cherkauer, K. A., and D. P. Lettenmaier, 1999: Hydrologic effects of frozen soils in the upper Mississippi River basin. *J. Geophys. Res.*, **104**, 19599-19,610, https://doi.org/10.1029/1999JD900337.

——, L. C. Bowling, and D. P. Lettenmaier, 2003: Variable infiltration capacity cold land process model updates. *Glob. Planet. Change*, **38**, 151–159, https://doi.org/10.1016/S0921-8181(03)00025-0.

Clarke, G. K. C., A. H. Jarosch, F. S. Anslow, V. Radić, and B. Menounos, 2015: Projected deglaciation of western Canada in the twenty-first century. *Nat. Geosci.*, **8**, 372–377, https://doi.org/10.1038/ngeo2407.

Cuffey, K. M., and W. S. B. Paterson, 2010: *The Physics of Glaciers*. Academic Press, 722 pp.

Dadic, R., R. Mott, M. Lehning, and P. Burlando, 2010: Wind influence on snow depth distribution and accumulation over glaciers. *J. Geophys. Res. Earth Surf.*, **115**, F01012, https://doi.org/10.1029/2009JF001261.

Elder, K., 1995: Modeling the spatial distribution of seasonal snow accumulation on Teton Glacier, Wyoming, USA. *Biogeochemistry of Seasonally Snow-Covered Catchments (Proceedings of a Boulder Symposium, July 1995)*, *IAHS Publ.*, IAHS Press.

Grabiec, M., D. Puczko, T. Budzik, and G. Gajek, 2011: Snow distribution patterns on Svalbard glaciers derived from radio-echo soundings. *Pol. Polar Res.*, **32**, 393–421, https://doi.org/10.2478/v10183-011-0026-4.

Gruber, S., 2007: A mass-conserving fast algorithm to parameterize gravitational transport and deposition using digital elevation models. *Water Resour. Res.*, **43**, W06412, https://doi.org/10.1029/2006WR004868.

Herron, M. M., and C. C. Langway, 1980: Firn densification: An empirical model. *J. Glaciol.*, **25**, 373–385.

Iooss, B., A. Janon, and G. Pujol, 2019: *sensitivity: Global Sensitivity Analysis of Model Outputs*.

Jarosch, A. H., C. G. Schoof, and F. S. Anslow, 2013: Restoring mass conservation to shallow ice flow models over complex terrain. *The Cryosphere*, **7**, 229–240, https://doi.org/10.5194/tc-7-229-2013.

Kienzle, S. W., 2008: A new temperature based method to separate rain and snow. *Hydrol. Process.*, **22**, 5067–5085, https://doi.org/10.1002/hyp.7131.

Klok, E. J. L., and J. Oerlemans, 2002: Model study of the spatial distribution of the energy and mass balance of Morteratschgletscher, Switzerland. *J. Glaciol.*, **48**, 505–518, https://doi.org/10.3189/172756502781831133.

Kuhn, M., 2003: Redistribution of snow and glacier mass balance from a hydrometeorological model. *J. Hydrol.*, **282**, 95–103, https://doi.org/10.1016/S0022-1694(03)00256-7.

Liang, X., D. P. Lettenmaier, E. F. Wood, and S. J. Burges, 1994: A simple hydrologically based model of land-surface water and energy fluxes for general-circulation models. *J. Geophys. Res.-Atmospheres*, **99**, 14415–14428, https://doi.org/10.1029/94JD00483.

Liang, X., E. F. Wood, and D. P. Lettenmaier, 1996: Surface soil moisture parameterization of the VIC-2L model: Evaluation and modification. *Glob. Planet. Change*, **13**, 195–206, https://doi.org/10.1016/0921-8181(95)00046-1.

——, ——, and ——, 1999: Modeling ground heat flux in land surface parameterization schemes. *J. Geophys. Res. Atmospheres*, **104**, 9581–9600, https://doi.org/10.1029/98JD02307.

Moore, R. D., S. W. Fleming, B. Menounos, R. Wheate, A. Fountain, K. Stahl, K. Holm, and M. Jakob, 2009: Glacier change in western North America: influences on hydrology, geomorphic hazards and water quality. *Hydrol. Process.*, **23**, 42–61, https://doi.org/10.1002/hyp.7162.

Paterson, W. S. B., 1994: *The Physics of Glaciers*. Third Edition. Butterworth-Heinemann, 496 pp.

Roe, G. H., 2004: Orographic precipitation. *Annu. Rev. Earth Planet. Sci.*, **33**, 645–671, https://doi.org/10.1146/annurev.earth.33.092203.122541.

Saltelli, A., 2002: Making best use of model evaluations to compute sensitivity indices. *Comput. Phys. Commun.*, **145**, 280–297, https://doi.org/10.1016/S0010-4655(02)00280-1.

Schnorbus, M., K. Bennett, and A. Werner, 2010: *Quantifying the water resource impacts of mountain pine beetle and associated salvage harvest operations across a range of watershed scales: Hydrologic modelling of the Fraser River basin.* Canadian Forest Service, Pacific Forestry Centre, http://www.cfs.nrcan.gc.ca/pubwarehouse/pdfs/31207.pdf.

Schnorbus, M. A., 2018: *VIC Glacier (VIC-GL): Modelling Glacier Dynamics with the HydroConductor Model*. VIC Generation 2 Deployment Report, Volume 2, Pacific Climate Impacts Consortium, University of Victoria, Victoria, BC., 27 pp.

Stahl, K., R. D. Moore, J. M. Shea, D. Hutchinson, and A. J. Cannon, 2008: Coupled modelling of glacier and streamflow response to future climate scenarios. *Water Resour. Res.*, **44**, W02422, https://doi.org/10.1029/2007WR005956.

Stone, J., 2013: *Variable Infiltration Capacity Software Improvements*. Pacific Climate Impacts Consortium and Faculty of Engineering, 35 pp.

Sun, S., J. Jin, and Y. Xue, 1999: A simple snow-atmosphere-soil transfer model. *J. Geophys. Res. Atmospheres*, **104**, 19587–19597, https://doi.org/10.1029/1999JD900305.

USACE, 1956: *Snow hydrology: Summary report of the snow investigations*. North Pacific Division, US Army Corps of Engineers,.

Wheler, B. A., and G. E. Flowers, 2011: Glacier subsurface heat-flux characterizations for energy-balance modelling in the Donjek Range, southwest Yukon, Canada. *J. Glaciol.*, **57**, 121–133, https://doi.org/10.3189/002214311795306709.